

RA. 1238

HNS-1/2

c.1

# NATIONAL ADVISORY COMMITTEE FOR AERONAUTICS

TECHNICAL NOTE

No. 1266

APR 28 1947

FLIGHT MEASUREMENTS OF HELICOPTER BLADE MOTION  
WITH A COMPARISON BETWEEN THEORETICAL  
AND EXPERIMENTAL RESULTS

By Garry C. Myers, Jr.

Langley Memorial Aeronautical Laboratory  
Langley Field, Va.

**FOR REFERENCE**

---

NOT TO BE TAKEN FROM THIS ROOM



Washington

April 1947

**NACA LIBRARY**  
LANGLEY MEMORIAL AERONAUTICAL  
LABORATORY  
Langley Field, Va.

## NATIONAL ADVISORY COMMITTEE FOR AERONAUTICS

## TECHNICAL NOTE NO. 1266

## FLIGHT MEASUREMENTS OF HELICOPTER BLADE MOTION

## WITH A COMPARISON BETWEEN THEORETICAL

## AND EXPERIMENTAL RESULTS

By Garry C. Myers, Jr.

## SUMMARY

In order to provide basic data on helicopter rotor-blade motion, photographic records of the behavior of a blade in flight were obtained with a conventional single-rotor helicopter. The results of measurements of flapping motion, in-plane motion, and blade distortions are presented for selected conditions of flight at tip-speed ratios ranging from 0.12 to 0.25. The flapping and in-plane measurements were reduced to Fourier series coefficients and are presented in tabular form. Values of measured flapping motion were compared with theoretically calculated values, and agreement was found to be good enough to render the theory useful, within the range of conditions tested, in such problems as estimation of control displacement for trim and static-stability determination and in the design of the rotor hub. The largest deviations between predicted and measured flapping motion were noted in the rather limited climb conditions tested and further examination of this deviation appears desirable.

Periodic in-plane motion due to air forces was shown to be small, having an amplitude of about  $1^\circ$  at a tip-speed ratio of 0.25. This fact simplifies the design problem involved in minimizing damper loads. The mean drag angle is found to be proportional (within  $\pm 3$  percent) to the rotor torque divided by the square of the rotational speed over a wide range of flight conditions, which suggests the use of the drag angle in devising a simple service torquemeter for the helicopter. The agreement between measured and predicted drag angles is considered adequate to warrant confidence in the predicted values in designing the rotor hub.

Plots of blade twisting and blade bending in the plane of flapping are presented for a sample case. The outer quarter of the blade was concave downward during most of or all of each revolution for every condition examined, which indicates the need for including tip-loss factors in blade-stress calculations.

## INTRODUCTION

The ability to predict the motion of the blades of a flapping rotor is of fundamental importance in the solution of many rotary-wing problems. Information on blade-flapping motion is, for example, an important step in studies of rotor stability, since the orientation of the rotor disk must be known with respect to known axes. For the same reason, an understanding of the flapping motion provides a basis for the prediction of required control displacements for trim. A knowledge of in-plane motion and blade distortions is essential to studies of blade stresses and rotor vibration. Ability to predict blade motion is also necessary for the rational design of the rotor hub, specifically the stop settings and bearing positions.

Although much experimental and theoretical blade-motion data are available for autogiros, little data have been published for the power-on helicopter condition. Blade-motion theory as presented in reference 1 is equally applicable to power-on and autorotative flight conditions but, because of the difference in the direction of flow through the disk and the accompanying changes in distribution of applied forces, use of correction factors for the helicopter condition as determined from comparisons of theoretical and experimental autogiro data is questionable. In view of these facts, a test program was started to obtain data on helicopter blade motion. The present paper gives results obtained in selected conditions of flight. The tests were conducted in the Flight Research Division of the Langley Memorial Aeronautical Laboratory.

Measurements of flapping and in-plane motion in terms of Fourier series coefficients obtained by harmonic analysis are presented herein along with sample blade-twist and bending measurements. The measured flapping values are used as an experimental check on rotor theory in order to determine the usefulness of the theory for various applications. By establishing the degree of agreement between theoretical and experimental data, the experimental data not only indicate the accuracy with which theory may be used for flapping predictions but also aid in checking the adequacy of some of the assumptions used in all phases of rotor theory. The magnitudes and trends of the higher harmonics of flapping and the periodic in-plane motion are studied as a source of rotor vibration. Measurements of blade twisting and bending are examined with a view to aiding in the determination of some of the factors affecting the disposition of forces on the rotor blade in flight.

Although by no means exhaustive, the data presented are felt to be of great fundamental value in defining the actual nature of helicopter blade motion.

## DEFINITIONS AND SYMBOLS

The terms "feathering" and "cyclic-pitch variation" as used herein refer to the variation of rotor-blade pitch angle with blade azimuth position.

The "axis of no feathering" is the axis about which there is no first-harmonic feathering or cyclic-pitch variation. (See the appendix for a detailed explanation of the use of this axis.)

$\psi$  blade azimuth angle measured from down-wind position in the direction of rotation

$\beta_s$  observed blade flapping angle; angle between the blade and the plane perpendicular to the rotor-shaft axis expressed as a function of azimuth angle  $\psi$  by the Fourier series

$$\beta_s = a_{0s} - a_{1s} \cos \psi - b_{1s} \sin \psi - a_{2s} \cos 2\psi - b_{2s} \sin 2\psi \dots$$

$\beta$  blade flapping angle; angle between blade and the plane perpendicular to the axis of no feathering expressed as a function of azimuth angle  $\psi$  by the Fourier series

$$\beta = a_0 - a_1 \cos \psi - b_1 \sin \psi - a_2 \cos 2\psi - b_2 \sin 2\psi \dots$$

$\theta_s$  instantaneous blade pitch angle at the 0.75 radius measured with respect to the plane perpendicular to the rotor-shaft axis expressed as a function of the azimuth angle  $\psi$  by the Fourier series

$$\theta_s = A_{0s} - A_{1s} \cos \psi - B_{1s} \sin \psi - A_{2s} \cos 2\psi - B_{2s} \sin 2\psi \dots$$

$\theta$  instantaneous blade pitch angle at the 0.75 radius measured with respect to the axis of no feathering expressed as a function of the azimuth angle  $\psi$  by the Fourier series

$$\theta = A_0 - A_2 \cos 2\psi - B_2 \sin 2\psi \dots$$

$\zeta$  blade drag angle; angle between blade and a line drawn through the center of rotation and drag hinge (vertical pin), positive in the direction of rotation, expressed as a function of azimuth angle by the Fourier series

$$\zeta = \zeta_0 + E_1 \cos \psi + F_1 \sin \psi + E_2 \cos 2\psi + F_2 \sin 2\psi \dots$$

- V true airspeed of helicopter, miles per hour
- $\mu$  tip-speed ratio  $\left( \frac{V \cos \alpha}{\Omega R} \right)$
- $\lambda$  inflow ratio  $\left( \frac{V \sin \alpha + v}{\Omega R} \right)$
- v induced velocity at the rotor
- $\alpha$  rotor angle of attack; angle between the projection of the axis of no feathering in the plane of symmetry and a line perpendicular to the flight path, positive when axis is pointing rearward, degrees
- $\alpha_f$  fuselage angle of attack; angle between relative wind and a line in the plane of symmetry and perpendicular to the main-rotor-shaft axis, degrees
- $C_T$  thrust coefficient  $\left( \frac{T}{\rho \pi R^2 (\Omega R)^2} \right)$
- T rotor thrust, pounds (assumed equal to  $L/\cos \alpha$ )
- L rotor lift, pounds
- $\rho$  mass density of air, slugs per cubic foot
- $\Omega$  rotor angular velocity, radians per second
- R rotor-blade radius, feet
- P/L shaft power drag-lift ratio; ratio of drag equivalent of main-rotor-shaft power absorbed at a given airspeed to rotor lift ( $Q_0/VL$ )
- Q shaft torque, pound-feet
- $\sigma$  solidity  $\left( \frac{bc_e}{\pi R} \right)$
- $c_e$  equivalent chord, feet  $\left( \frac{\int_0^R cr^2 dr}{\int_0^R r^2 dr} \right)$
- c local chord, feet
- r radius to blade element, feet

- $\gamma$  mass constant of rotor blade  $\left( \frac{c_{\ell} \rho a R^4}{I_1} \right)$ ; ratio of air forces  
to centrifugal forces  
(mass)  
b number of blades  
 $I_1$  mass moment of inertia of rotor blade about flapping hinge  
a slope of lift coefficient against section angle of attack,  
per radian (assumed equal to 5.73 in present paper)  
B tip-loss factor (taken as 0.97 in present paper)  
Subscript:  
s referred to rotor-shaft axis

#### APPARATUS AND METHODS

The helicopter used in the present tests was the Sikorsky HNS-1 (Army YR-4B) equipped with the original production rotor blades. The blade plan form, pertinent dimensions, and mass characteristics are presented in figure 1. The instrument installation was that described in detail in reference 2 in addition to a 35-millimeter motion-picture camera mounted rigidly on the rotor hub and pointed out along one blade as shown in figure 2.

The blade was marked in such a way as to identify the 0.75 radius and several other spanwise stations. Targets were mounted ahead of and behind the blade at the 0.75 radius to permit pitch-angle measurements.

Typical photographs obtained in flight are shown as figure 3. Blade motion was determined by observing the manner in which the blade moved in the field of the camera which was fixed relative to the rotor shaft. This motion was interpreted in terms of angles and deflections from similar photographs taken on the ground with the blade kept straight by means of a beam and wedges and held at known positions in space. The flapping and in-plane motion of the blade was defined as the motion of a line connecting the blade root and 0.75 radius.

The azimuth positions of the camera and blade were determined by using the tail rotor as a fixed reference. Orientation in azimuth of camera frames between those in which the tail rotor appeared was determined by assuming constant rotor-shaft and camera-

film speeds over the interval. Frames were oriented in azimuth to a precision of  $\pm 2^\circ$ .

Flight tests consisted of a series of level-flight runs and some sample glides and climbs. The level-flight runs covered an airspeed range from 43 to 73 miles per hour at fixed rotational speeds and covered three rotational speeds at each end of the forward-speed range. Simultaneous records were taken with the camera and with the recording instruments used for recording the flight conditions.

A sample of the data obtained from the camera records is given in figure 4, which shows results from a typical test consisting of about 200 blade positions and covering about 20 revolutions. Reading accuracy for the flapping, in-plane, and pitch angles was within  $\pm 0.1^\circ$  and for the tip deflections, within  $\pm 0.1$  inch. The consistency of the test points in forming a single curve for the bending measurements suggests that the scatter evident in the flapping and pitch measurements may be due chiefly to the failure of the rotor blade to retrace its path in successive revolutions. The camera may be considered rigidly supported insofar as flapping, bending, and pitch measurements are concerned. In the in-plane direction, however, play in the crown-housing attachment permitted the camera to be rotated as much as  $\pm 0.4^\circ$ . The control-linkage and blade pitching-moment characteristics provide a moment which tends to hold the crown-housing at one end of its free travel, and the small scatter in individual runs and in cross-plots of coefficients indicate that the play was suppressed. This possible source of inaccuracy, however, should be kept in mind in interpreting the dragging-motion measurements.

## RESULTS AND DISCUSSION

For discussion and analysis of the test results, the subject can be divided into three parts: flapping motion, in-plane motion, and blade distortions.

### Flapping Motion

The flapping and feathering data obtained in flight are summarized in table I. Values are given that determine the flight condition, the measured flapping motion (that is, the flapping motion of the blade with respect to the shaft), and the measured

feathering motion (that is, the cyclic-pitch variation with respect to the shaft, due primarily to the control setting). The measured flapping and feathering values are presented in terms of Fourier series coefficients obtained by harmonic analysis of the flapping and pitch-angle data.

Reduction of data to pure flapping system.- In order to compare the measured flapping motions with theoretical predictions, the actual flapping-feathering system was reduced to an equivalent pure flapping system. Flapping was referred to an axis about which there was no first-harmonic cyclic-pitch variation, which has been defined as the axis of no feathering. The simple conversions of measured flapping and feathering coefficients to the flapping coefficients referred to the axis of no feathering are given in the appendix. The flapping coefficients referred to the axis of no feathering are given in table I.

Theoretical calculations.- Flapping coefficients were calculated using the performance charts of reference 3 in conjunction with the thrust and flapping-motion equations of reference 1. Calculations were made using experimental values of the performance parameters  $C_T/\sigma$ ,  $\mu$ , and  $P/L$ . Since the theoretical expressions for the flapping coefficients are given in reference 1 in terms of the variables  $\lambda$ ,  $\theta$ , and  $\mu$ , it was first necessary to determine  $\lambda$  and  $\theta$  for the given conditions. The variable  $\theta$  was determined from the charts of reference 3 which define  $\theta$  for given values of  $P/L$ ,  $\mu$ , and  $C_T/\sigma$  and for a fixed profile-drag polar. With the value of  $\theta$  known,  $\lambda$  was obtained from equation (6) of reference 1 which relates  $C_T/\sigma$ ,  $\lambda$ ,  $\theta$ , and  $\mu$ .

Calculations for level flight were made for three groups of  $C_T$  corresponding to the three rotational speeds for which data were obtained in flight. For each value of  $C_T$ , the variation of  $P/L$  with  $\mu$  was obtained by fairing through the experimental values with a theoretical variation of  $P/L$  with  $\mu$  used as a guide. For the glide and climb conditions, theoretical values of the flapping coefficients were calculated for the actual flight conditions measured in each case.

Significance of Fourier series coefficients.- For the purpose of analysis, the flapping motion is examined in terms of the coefficients of the following Fourier series:

$$\beta = a_0 - a_1 \cos \psi - b_1 \sin \psi - a_2 \cos 2\psi - b_2 \sin 2\psi \dots$$

Physically, these coefficients represent the amplitudes of the sinusoidal motions which, when added, will produce the actual



flapping motion. The coefficient  $a_0$ , for example, represents the steady coning angle. The coefficient  $a_1$  represents the amplitude of rearward tilt of the disk with respect to the axis of no feathering, and  $b_1$  represents the degree to which the disk is tilted laterally toward the advancing side. The higher harmonics,  $a_2$ ,  $b_2$ ,  $a_3$ , and so forth determine the departure of the three-quarter-radius station from a plane. Although these higher-harmonic coefficients are quite small, they are significant in studies of rotor vibration.

Comparison of theoretical results with experimental results for level flight.—The flight values of the flapping coefficients and pitch angle for the level-flight conditions are compared with theory in figure 5. The measured coefficients for each of the groups of  $C_T$  were adjusted to mean values ( $C_T = 0.0046$ ,  $0.0055$ , and  $0.0063$ ) using an increment based on the calculated variation of flapping coefficient with  $C_T$ . Although the adjustments were small and did not alter the results materially, they did reduce the scatter in the data in every case.

In figure 5(a) measured and calculated coning angles are seen to be in good agreement;  $a_0$  was underestimated by less than  $1/2^\circ$ . The theory is thus seen to predict closely the average radial center-of-pressure position. The variations of the coning angle with  $\mu$  and  $C_T$  are quite well predicted except for the higher values. In this connection, the observations of stalling on the retreating blade are pertinent. Various degrees of tip stalling were observed at higher speeds and high thrust coefficients, and at the highest measured value of  $\mu$  ( $0.25$ ), the tip of the blade was stalled for approximately one-fourth of each revolution. Stalling measurements for these speeds and thrust coefficients are presented and discussed in reference 4. The test point for  $\mu = 0.25$  represents a condition of severe stall. A definite decrease in coning angle, as compared with the trend of the rest of the data, is shown in the figure for this condition. This decrease is presumably due to the loss of lift on the retreating tip resulting from stall.

In figure 5(b), the longitudinal flapping coefficient  $a_1$  is also seen to be underestimated; the disagreement becomes larger at the higher values of  $\mu$  and  $C_T$ . This increase in disagreement with increasing values of  $\mu$  and  $C_T$  might be accounted for by the increasing region of angles of attack on the retreating side that fall above the linear portion of the lift curve. With the exception of the condition for severe stalling, the predicted and measured values differ by less than  $1^\circ$ .

The lateral flapping coefficient  $b_1$  in figure 5(c) is underestimated, as might be expected since no account is taken in the calculations of the nonuniformity of inflow over the disk in the direction of flight. If a linear variation of inflow is assumed instead of uniform inflow, agreement is considerably improved. The curve in figure 5(c) for linearly varying inflow was calculated using the following equation (reference 5):

$$\Delta b_1 = \frac{B^2}{B^2 + \frac{1}{2}\mu^2} \frac{KC_T}{2(\mu^2 + \lambda^2)^{1/2}} \quad (1)$$

where  $K + 1$  is the ratio of the induced velocity at the rear of the disk to the mean induced velocity, with a linear variation from front to rear assumed. The value of  $K$  used was computed using the tangent approximation of figure 3 of reference 6. The resulting curve differs from the corresponding test points by less than 1%. It appears possible that the greater part of the remaining discrepancy can be accounted for by more refined treatments of the effects of induced flow patterns.

The coefficients  $a_2$  and  $b_2$  are small as shown in figure 5(d) and, although the agreement is poor on a percentage basis, the order of magnitude and variations of coning angle with  $C_T$  and  $\mu$  are quite satisfactory. The effects of stall are again evident in the test point for  $\mu = 0.25$ . It should be pointed out that the presence of some second-harmonic feathering (see table I) necessarily affected the second-harmonic flapping values. These higher harmonics of feathering result from play and nonlinearity in the blade-feathering linkage and from periodic blade twisting. Examination of the problem leads to the opinion, however, that the degree of agreement shown would not be significantly affected by application of a correction to the measured flapping for the effect of this feathering. The measured third harmonics  $a_3$  and  $b_3$  are presented in figure 5(e). No theoretical values are given since the equations used extended only through the second harmonics. The third harmonics are seen to be quite small. (The scale is five times that for  $a_2$  and  $b_2$ .)

The abrupt increase in the second and third harmonics in the condition of extreme stall is interesting in connection with the pilot's reports of severe vibration in the highly stalled condition.

In figure 5(f) the calculated value of mean pitch angle is compared with the theoretical value. The coefficient  $A_0$  is seen

to be overestimated by an appreciable amount, which indicates that the assumed lift-curve slope is too low. Agreement is improved at higher tip-speed ratios, which again may be the result of an effectively decreased lift-curve slope caused by the increasing regions of high angle of attack. Also, as will be shown in the section of the present paper entitled "Effect of profile drag" part of the disagreement arises from the optimistic profile-drag values assumed in the calculations.

Comparison of theoretical results with experimental results for climbs and glides.- In view of the limited data available for the climb and glide conditions and the difficulty of presenting a comparison of calculated and measured flapping coefficients for climb on a single plot, the coefficients for these conditions are given along with calculated values in table XI.

Examination of table II, together with the level-flight comparison of figure 5, shows how the degree of agreement between theory and experiment is affected by flight condition. In general, agreement is better for glides and poorer for climbs than for level flight. Theory appears to underpredict the rate of change of the coefficients with  $P/L$ . This discrepancy in trend is not felt to be large enough to impair seriously the general usefulness of the theory but is considered to warrant further investigation.

Effect of profile drag.- In the theoretical calculations, one approximation in addition to the assumptions governing the general theoretical equations was made. The profile drag of the blades tested was assumed to be represented by the polar on which the performance charts of reference 3 are based. Both performance measurements of the actual rotor and wind-tunnel tests on a portion of a similar blade indicate that the profile drag was actually much higher than that assumed. Accordingly, sample calculations were made assuming a drag polar with 30 percent higher profile drag to determine the effects of the assumed profile drag. The effects on the predicted flapping coefficients were very small and the 30-percent increase in profile drag resulted in a change of less than 2 percent in the coefficients. The predicted value of  $A_j$  was decreased about  $0.4^\circ$ , however, which improved the agreement between calculated and measured values (fig. 5(f)) appreciably.

General remarks.- In order to illustrate more clearly the over-all agreement between calculated and measured flapping, the resultant flapping motions as calculated and as measured for a sample case are compared in figure 6. The maximum discrepancy

is seen to be about  $1\frac{1}{2}^{\circ}$ , which is small enough to warrant the use of the theoretical coning angle and flapping motion in designing the rotor hub.

The agreement between the theoretical and measured longitudinal and lateral flapping angles (shown in fig. 5 to be within  $1^{\circ}$ ) is considered to justify use of the theory for the solution of problems in which a knowledge of the orientation of the plane of the 0.75 radius under different conditions is desired. For example, the orientation of the plane of the rotor disk must be known in predictions of control required for trim and in the design of the rotor hub.

In connection with helicopter static stability, the rates of change of the lateral and longitudinal flapping angles with thrust coefficient and tip-speed ratio are significant. The experimental and theoretical trends shown in figure 5 are felt to be in sufficient agreement to indicate that the theory will prove useful in the study of helicopter static stability, at least for preliminary examination of the problems involved. In arriving at this conclusion, the effect of adjusting the values of the flapping coefficients to constant-power conditions was examined.

In connection with stability studies, it should be mentioned that knowledge of the orientation of the plane of the 0.75 radius does not strictly define the direction of the rotor resultant force. Available theoretical treatments and experimental results indicate that, in connection with the stability and control studies referred to, the error involved in ignoring the component of the resultant force in the plane of rotation is, in general, not significant. A full discussion of this point is felt to be beyond the scope of the present paper.

#### In-Plane Motion

Measured values of blade in-plane motion for each flight condition are given in table III in terms of the Fourier series coefficients  $\zeta_0$ ,  $E$ , and  $F$ , where

$$\zeta = \zeta_0 + E_1 \cos \psi + F_1 \sin \psi + E_2 \cos 2\psi + F_2 \sin 2\psi + \dots \quad (2)$$

and where  $\zeta$  is the angle between the blade axis and a line through the axis of rotation and the drag hinge. The drag hinge is the vertical pin which allows the blade freedom of motion in the plane of the disk.

Periodic in-plane motion.- Periodic in-plane motion arises from two sources - air forces and "mechanical forces." The term "mechanical forces" as used herein represents the in-plane forces due to the changing moment of inertia during each revolution of the flapping blade with respect to its shaft.

Fourier series coefficients obtained from harmonic analysis of the measured periodic in-plane motion were calculated in order to determine the magnitudes of the various harmonics. Since the "mechanical" part of the in-plane motion, caused by first-harmonic flapping with respect to the shaft, is a function of fuselage center-of-gravity position and fuselage pitching moments and has no fundamental significance, this motion, as calculated from angular momentum considerations (using the treatment of reference 7), was subtracted from the first-harmonic coefficients in order to study the remaining in-plane motion caused by air forces. The motion due to air forces was found to have a relatively small amplitude over the entire range of conditions tested and to reach a maximum of about  $1^\circ$  at a tip-speed ratio of 0.25.

The measured periodic in-plane motion has been plotted for a sample case in figure 7, along with the motion due to air forces alone. The motion due to air forces alone was determined by subtracting the calculated "mechanical" contribution to the motion from the measured motion. It may be noted that the maximum air-force contributions to the periodic in-plane motion occur at approximately  $\psi = 170^\circ$  and  $\psi = 350^\circ$ .

As has been pointed out, the phase and amplitude of the "mechanical" input depend upon the flapping motion relative to the shaft. For the condition shown in figure 7, the "mechanical" input is seen to add to the air-force input. The "mechanical" input may be varied by changing the combination of shaft angle and control position, through use of a horizontal control surface for example or by variation of the fuselage center-of-gravity position. The changes in "mechanical" input with normal fuselage center-of-gravity variations may result in motions of the order of  $3^\circ$  to  $4^\circ$  which are large with respect to the air-force input. Since the "mechanical" input is under the designer's control, design center-of-gravity positions (relative to the shaft) may be chosen so as to offset to a large degree the motion due to air forces and thus blade in-plane stresses and vibrations in the helicopter due to damper loads may be reduced.

Mean drag angle.- The mean drag angle in radians is given approximately by the expression

$$\xi_0 = - \frac{Q}{be(M_0^2 r_{cg}) \left( \frac{e}{r_{df}} + 1 \right)} \quad (3)$$

where

- Q    main-rotor-shaft torque input, pound-feet
- b    number of blades
- e    distance from drag hinge (vertical pin) to axis of rotation,  
      feet
- M    blade mass, slugs
- $r_{cg}$    radial position of blade center of gravity, feet; measured  
      from drag hinge
- $r_{df}$    radial position of resultant drag force, feet; measured  
      from drag hinge

Equation (3) indicates that for a given rotor the mean drag angle is essentially a function of  $Q/\Omega^2$ . Since the radial position of the resultant aerodynamic force  $r_{df}$  is very large with respect to e ( $r_{df}$  is on the order of  $0.7R$ ), the drag angle should be relatively insensitive to changes in  $r_{df}$ . For example, when  $r_{df} = 0.7R$ , a  $\pm 30$ -percent variation in  $r_{df}$  in equation (3) produces only a  $\pm 2$ -percent change in  $\xi_0$ .

In figure 8, measured values of the ratio of the rotor-shaft power to the cube of the rotor rotational speed (proportional to  $Q/\Omega^2$ ) are plotted against measured drag angles. The test points represent a variety of conditions of flight including level flight from the speed for minimum power to top speed, climbs, and autorotation. It is seen that excellent correlation exists; the maximum scatter is about 3 percent from a mean straight line, which is the order of accuracy of the measurements. The linearity of these data suggests that the theoretical relation should be useful in interpreting drag angle in terms of main-rotor-shaft torque. A mechanical device which indicated the mean drag angle would provide a simple means of indicating changes in power absorbed by the main rotor and, if calibrated, could be used as a service torquemeter. If a probable representative value of the radial position of the resultant aerodynamic drag force is assumed, such as  $0.6R$  or  $0.8R$ , the drag angles for the various power conditions can be predicted from equation (3) to within about  $1/2^\circ$ . This approach thus appears to be accurate enough to be useful in designing the rotor hub.

### Blade Distortions

Blade twisting.- Sample measurements of blade torsional deformation were made for an extreme case, a velocity of 70 miles per hour at which a large area of stall was encountered. Values for twist occurring between two stations were obtained by measuring the angle of the 0.75-radius targets relative to the center chordwise strip at the 0.50 radius. (See fig. 3.) These values are plotted against azimuth angle in figure 9. The measurements are of interest in that they isolate the twisting caused by the air forces on the outer part of the blade. The periodic twist is seen to be of the order of  $\pm 1/3^\circ$  with about  $-0.1^\circ$  mean twist. Approximate calculations indicate that in order to produce  $\pm 1/3^\circ$  twist a center-of-pressure travel of the order of  $\pm 1.5$  percent of the chord is required and that the mean twist corresponds to a displacement of the center of pressure from the center of gravity of about  $1/2$  percent of the chord. The effect of stalling and the associated diving moment on the blade twist is evidenced by the dip in the curve of figure 9 between approximately  $240^\circ$  and  $360^\circ$  azimuth.

The twisting-down on the advancing side (high velocities and low angles) together with the twisting-up on the retreating side (low velocities and high angles) suggests that the blade center of gravity is behind the aerodynamic center and that an appreciable diving-moment coefficient exists about the aerodynamic center. Some diving moment would be expected on the blades tested due to camber caused by fabric distortion.

Blade bending.- In figure 10, blade-bending deflection curves are shown for several azimuth positions in a sample case (70 mph, 225 rotor rpm). Deflections are given relative to a straight line through the hub and the 0.75 radius. The figure indicates that the tip portion of the blade is bent concave downward over the greater part of the disk, which gives an S-shape curve to the spar. Inasmuch as the spanwise mass distribution for the blades tested was approximately proportional to the chord with no concentrated masses along the span, this bending indicates a definite loss of lift at the blade tips. Corresponding observations for other flight conditions likewise showed this S-shape curve. Since computations making no allowance for tip losses indicate appreciable concavity upward over the entire blade, it thus appears that tip losses must be allowed for in-blade bending-stress calculations in order to obtain reasonably accurate answers. This indication is in agreement with the conclusions arrived at in the theoretical examination of tip-loss effects given in reference 8.

A violent flipping-up of the outer part of the blade will be noted in figure 10 in the region of  $270^\circ$  azimuth, that is, on the retreating side of the disk. The nature of this motion is more clearly shown in the sample bending data in figure 4. The cause of this phenomenon is not fully understood at the present time and requires further investigation. There are indications that it may involve an instability due to rearward chordwise center-of-gravity position.

### CONCLUSIONS

On the basis of blade-motion measurements obtained on a helicopter in flight at tip-speed ratios ranging from 0.12 to 0.25, the following conclusions are drawn:

1. Comparisons of measured and calculated flapping motions indicated that, for the range of level-flight conditions tested, the coning angle and the longitudinal and lateral flapping angles may be predicted within about  $1^\circ$ , which renders predictions quite useful in the design of the rotor hub and for estimations of required control displacements for trim.
2. Somewhat larger deviations between predicted and measured flapping motion were noted in the rather limited climb conditions covered as compared with level-flight conditions, and further examination of this deviation appears desirable.
3. The predicted rates of change of the lateral and longitudinal flapping angles with tip-speed ratio and thrust coefficient were felt to be in sufficient agreement with the measured values to indicate that available blade-motion theory will prove useful in the study of helicopter static stability, at least for preliminary examination of the problems involved.
4. The periodic in-plane motion caused by air forces were small, having an amplitude of about  $1^\circ$  at a tip-speed ratio of 0.25. This fact simplifies the design problem involved in minimizing damper loads.
5. The mean drag angle was found to be proportional to the rotor-shaft torque divided by the square of the rotor angular velocity, within about  $\pm 3$  percent, over a wide range of flight conditions. The proportionality suggests use of the drag angle in devising a simple service torquemeter for the helicopter. The agreement between measured and predicted lag angles was considered adequate to warrant confidence in the predicted values in designing the rotor hub.



6. Measurements of blade distortions showed substantial downward bending of the outer quarter of the blade, presumably due to the loss of lift at the tip. It thus appears that tip losses must be allowed for in blade bending-stress calculations in order to obtain reasonably accurate answers.

Langley Memorial Aeronautical Laboratory  
National Advisory Committee for Aeronautics  
Langley Field, Va., February 20, 1947

## APPENDIX

CONVERSION OF MEASURED VALUES OF FEATHERING AND  
FLAPPING WITH RESPECT TO SHAFT TO FLAPPING  
ABOUT THE AXIS OF NO FEATHERING

Reason for conversion.- At the time that the basic theoretical treatments, such as that of reference 1, were made, the typical rotor arrangements involved the use of hinges to permit flapping but no mechanism by means of which feathering could be introduced with both flapping and feathering referred to the rotor shaft. The desired orientation of the rotor was achieved by tilting the rotor shaft. Since that time the mechanical arrangement in most designs has been altered so that the rotor attitude is controlled by feathering. In other words, a controllable amount of first-harmonic blade-pitch change is introduced relative to the axis of the rotor shaft. The two systems are aerodynamically equal; the blades follow the same path relative to space axes, as regards both pitch angle and flapping angle, for any given flight condition regardless of the mechanical means used for achieving it. This fact may be confirmed by inspection but has also been demonstrated mathematically in reference 9 and again in more detail in an unpublished analysis.

In practice, the present rotor systems, such as that of the helicopter tested, involve both flapping and feathering, and, for comparison with theory based on either the assumption of no feathering or no flapping, a conversion would be necessary. Since the available treatments, such as that in reference 1, assume no feathering, it is expedient to convert to this condition.

The conversion involved is simply a change of reference axes, which can be more easily understood by reference to figure 11. Figure 11(a) shows a longitudinal cross-section of the rotor cone for a system without feathering (that is, a pure flapping system) and the longitudinal tilt of the rotor shaft required to orient the rotor to correspond to some particular flight condition. In figure 11(b) the flight condition is assumed to be the same and hence the tilt of the rotor cone with respect to the flight path is the same, but the tilt is achieved by a combination of shaft tilt and feathering relative to this shaft. For clarity, the feathering is assumed to be achieved by a swash plate linked in such a manner that a  $1^\circ$  longitudinal tilt of the plate produces  $1^\circ$  of feathering in

the blades when the blades are in the lateral position and no feathering when the blades are aligned longitudinally. In other words, the blades do not change pitch while revolving, as referred to the plane of the swash plate, no matter how the swash plate is tilted. In figure 11(a) the blades do not change pitch as referred to the shaft axis while revolving. The axis of the swash plate in figure 11(b) is thus equivalent to the shaft axis in figure 11(a) insofar as periodic pitch-angle variation is concerned. Since the swash plate need not be rigged as assumed in this figure and since the true significance of its axis is that no feathering is introduced relative to it, this axis is termed the axis of no feathering, rather than the swash-plate axis. It corresponds to the shaft axis for an equivalent (or pure flapping) system incorporating no means for feathering.

A lateral cross-section of the rotor cone, similar to figure 11, may be drawn which would show the relationships between flapping and feathering in that plane.

Expressions for conversion.— The measured flapping (relative to shaft) is expressed as

$$\beta_s = a_{0s} - a_{1s} \cos \psi - b_{1s} \sin \psi - a_{2s} \cos 2\psi - b_{2s} \sin 2\psi \dots$$

The measured pitch angle (relative to shaft) is expressed as

$$\theta_s = A_{0s} - A_{1s} \cos \psi - B_{1s} \sin \psi - A_{2s} \cos 2\psi - B_{2s} \sin 2\psi \dots$$

Flapping with respect to the axis of no feathering is expressed as

$$\beta = a_0 - a_1 \cos \psi - b_1 \sin \psi - a_2 \cos 2\psi - b_2 \sin 2\psi \dots$$

Pitch angle with respect to the axis of no feathering is expressed as

$$\theta = A_0 - A_2 \cos 2\psi - B_2 \sin 2\psi \dots,$$

the first-harmonic terms becoming 0 by definition. Then the

equations for transferring from the shaft axis to the axis of no feathering are

$$a_0 = a_{0s}$$

$$a_1 = a_{1s} + B_{1s}$$

$$b_1 = b_{1s} - A_{1s}$$

$$a_2 = a_{2s}$$

$$b_2 = b_{2s}$$

$$A_0 = A_{0s}$$

$$A_2 = A_{2s}$$

$$A_3 = A_{3s}$$

If the angle between the perpendicular to the rotor shaft and the airstream is defined as  $\alpha_s$ , the rotor angle of attack  $\alpha$  is given by.

$$\alpha = \alpha_s - B_1$$

## REFERENCES

1. Bailey, F. J., Jr.: A Simplified Theoretical Method of Determining the Characteristics of a Lifting Rotor in Forward Flight. NACA Rep. No. 716, 1941.
2. Gustafson, F. B.: Flight Tests of the Sikorsky HNS-1 (Army YR-4B) Helicopter. I - Experimental Data on Level-Flight Performance with Original Rotor Blades. NACA MR No. L5C10, 1945.
3. Bailey, F. J., Jr., and Gustafson, F. B.: Charts for Estimation of the Characteristics of a Helicopter Rotor in Forward Flight. II - Profile Drag-Lift Ratio for Untwisted Rectangular Blades. NACA ACR No. L4H07, 1944.
4. Gustafson, F. B., and Myers, G. C., Jr.: Stalling of Helicopter Blades. NACA TN No. 3083, 1946.
5. Wheatley, John B.: An Aerodynamic Analysis of the Autogiro Rotor with a Comparison between Calculated and Experimental Results. NACA Rep. No. 487, 1934.
6. Coleman, Robert P., Feingold, Arnold M., and Stempin, Carl W.: Evaluation of the Induced-Velocity Field of an Idealized Helicopter Rotor. NACA ARR No. L5E10, 1945.
7. Wheatley, John B.: A Study of Autogiro Rotor-Blade Oscillations in the Plane of the Rotor Disk. NACA TN No. 581, 1936.
8. Duberg, John E., and Luecker, Arthur R.: Comparisons of Methods of Computing Bending Moments in Helicopter Rotor Blades in the Plane of Flapping. NACA ARR No. L5E23, 1945.
9. Lock, C. N. H.: Further Development of Autogyro Theory. Parts I and II. R. & M. No. 1127, British A.R.C., 1928.

TABLE I.- FLAPPING AND FEATHERING DATA

Exp.

Test run	V (mph)	Rotational speed of main rotor (rpm)	$\mu$	$C_T$	P/L	$a_{0s}$	$a_{1s}$	$b_{1s}$	$a_{2s}$	$b_{2s}$	$a_{3s}$	$b_{3s}$	$A_{0s}$	$A_{1s}$	$B_{1s}$	$A_{2s}$	$B_{2s}$	$A_{3s}$	$B_{3s}$	$\alpha_r$	$\alpha$	$a_1$	$b_1$
1	72.8	238	0.220	0.00486	0.281	7.81	0.99	0.30	0.32	-0.08	0.01	-0.01	9.03	-3.00	4.18	-0.16	-0.10	0.10	0.11	-7.4	-11.6	5.17	3.30
2	71.7	224	.230	.00545	.273	8.67	1.09	.41	.46	-.11	.02	-.04	10.10	-3.52	4.99	-.20	-.24	.11	.09	-6.9	-11.9	6.08	3.93
3	73.0	209	.249	.00631	.255	9.65	1.53	.81	.76	-.11	.11	.06	11.52	-4.01	6.36	-.28	.36	0	.02	-7.2	-13.6	7.89	4.82
4	58.6	225	.189	.00538	.240	8.30	.64	.68	.35	-.08	.02	-.01	8.17	-2.62	3.73	-.20	-.04	.03	.08	-4.5	-8.2	4.37	3.30
5	67.9	225	.217	.00542	.250	8.50	.99	.60	.44	-.09	.03	-.04	9.21	-2.83	4.57	-.14	-.10	.12	.02	-6.9	-11.5	5.56	3.43
6	50.5	225	.164	.00535	.260	8.18	.32	.56	.29	-.04	.04	-.04	7.63	-2.67	3.13	-.18	-.02	0	.09	-3.1	-6.2	3.45	3.23
7	43.7	223	.142	.00540	.264	8.16	.08	.55	.24	0	.04	-.04	7.11	-2.69	2.84	-.12	.01	.03	.12	-2.2	-5.0	2.92	3.24
8	43.1	241	.130	.00460	.313	7.10	.16	.45	.17	-.06	.05	-.05	6.28	-2.21	2.36	-.19	0	.04	.18	-2.3	-4.7	2.52	2.66
9	42.7	202	.153	.00656	.286	9.81	.12	.65	.32	-.07	.03	-.04	8.99	-3.17	4.03	-.14	-.04	-.03	.03	-2.0	-6.0	4.15	3.82
10	40.5	226	.128	.00531	.502	8.62	-.08	-.08	.28	-.11	.07	-.01	9.10	-3.22	3.50	-.15	.05	.09	.12	-9.7	-13.2	3.42	3.40
11	51.8	223	.166	.00546	.396	9.15	.13	.01	.33	-.10	.05	-.03	9.98	-3.55	4.10	-.12	.01	.08	.10	-10.1	-14.2	4.23	3.56
12	42.4	235	.130	.00407	.489	7.85	0	-.20	.14	-.07	.04	-.02	8.80	-2.82	3.13	-.18	.05	.05	.12	-9.5	-12.6	3.13	2.62
13	42.3	214	.141	.00588	.480	9.63	.14	.01	.36	-.11	.09	-.04	10.40	-3.49	4.26	-.20	-.01	.07	.09	-10.5	-14.8	4.40	3.50
14	43.0	221	.140	.00533	-.011	7.48	-.66	1.21	.10	-.11	.03	-.03	3.29	-1.58	2.33	.06	-.03	-.10	-.03	15.0	12.7	1.67	2.79
15	37.7	223	.119	.00549	-.012	7.55	-.63	1.16	.08	-.02	.02	0	3.43	-1.70	1.70	-.11	.04	-.11	.03	19.4	17.7	1.07	2.86

NATIONAL ADVISORY  
COMMITTEE FOR AERONAUTICS

TABLE II.- COMPARISON OF CALCULATED AND MEASURED

FLAPPING COEFFICIENTS IN GLIDES AND CLIMBS

Test run	Rate of climb (fpm)	V (mph)	$\mu$	$C_T$	P/L	$a_0$		$a_1$		$b_1$		$a_2$		$b_2$		$A_0$	
						Meas-ured	Calcu-lated	Meas-ured	Calcu-lated	Meas-ured	Calcu-lated	Meas-ured	Calcu-lated	Meas-ured	Calcu-lated	Meas-ured	Calcu-lated
10	468	40.5	0.128	0.00531	0.502	8.62	8.16	3.42	2.97	3.40	1.46	0.28	0.11	-0.11	-0.05	9.11	10.6
11	525	51.8	.166	.00546	.396	9.15	8.34	4.23	3.93	3.56	1.87	.33	.19	-.10	-.10	10.0	11.0
12	472	42.4	.130	.00487	.489	7.85	7.44	3.13	2.65	2.62	1.34	.14	.11	-.07	-.05	8.8	9.6
13	605	42.3	.141	.00588	.480	9.63	8.96	4.40	3.42	3.50	1.76	.36	.14	-.11	-.07	10.4	11.4
14	-1140	43.0	.140	.00533	-.011	7.48	7.30	1.67	1.99	2.79	1.40	.10	.11	-.11	-.04	3.3	4.7
15	-1260	37.7	.119	.00549	-.012	7.55	7.53	1.07	1.85	2.86	1.23	.08	.08	-.02	-.03	3.4	5.0

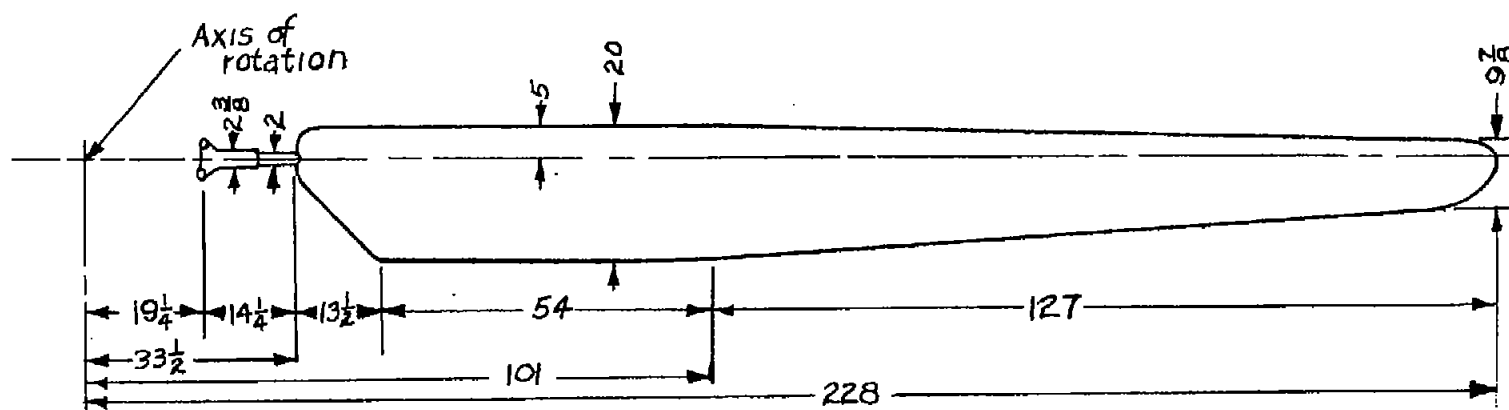
NATIONAL ADVISORY  
COMMITTEE FOR AERONAUTICS

TABLE III.- IN-PLANE-MOTION DATA

Test run	$\zeta_0$	$E_1$	$F_1$	$E_2$	$F_2$	$E_3$	$F_3$
1	-10.75	0.61	-0.49	-0.08	-0.08	0.12	0.02
2	-12.50	.79	-.60	-.03	-.08	.11	-.02
3	-14.72	1.11	-.88	-.02	-.13	.13	-.04
4	-8.83	.72	-.36	-.04	-.07	.11	-.02
5	-10.67	.75	-.49	-.07	-.05	.12	-.02
6	-8.18	.64	-.28	-.05	-.03	.12	-.01
7	-7.45	.57	-.23	-.04	-.03	.09	-.02
8	-6.80	.46	-.19	-.03	-.04	.13	.02
9	-10.39	.95	-.45	-.04	-.04	.10	-.06
10	-12.42	.55	-.33	-.05	-.04	.10	-.02
11	-13.03	.70	-.41	-.05	-.03	.09	-.01
12	-11.16	.44	-.28	-.07	-.04	.07	-.01
13	-14.5	.82	-.44	-.05	-.05	.07	-.01
14	-.09	.60	.08	0	-.02	.16	.11
15	-.03	.59	.09	-.02	-.04	.08	.18

NATIONAL ADVISORY  
COMMITTEE FOR AERONAUTICS.

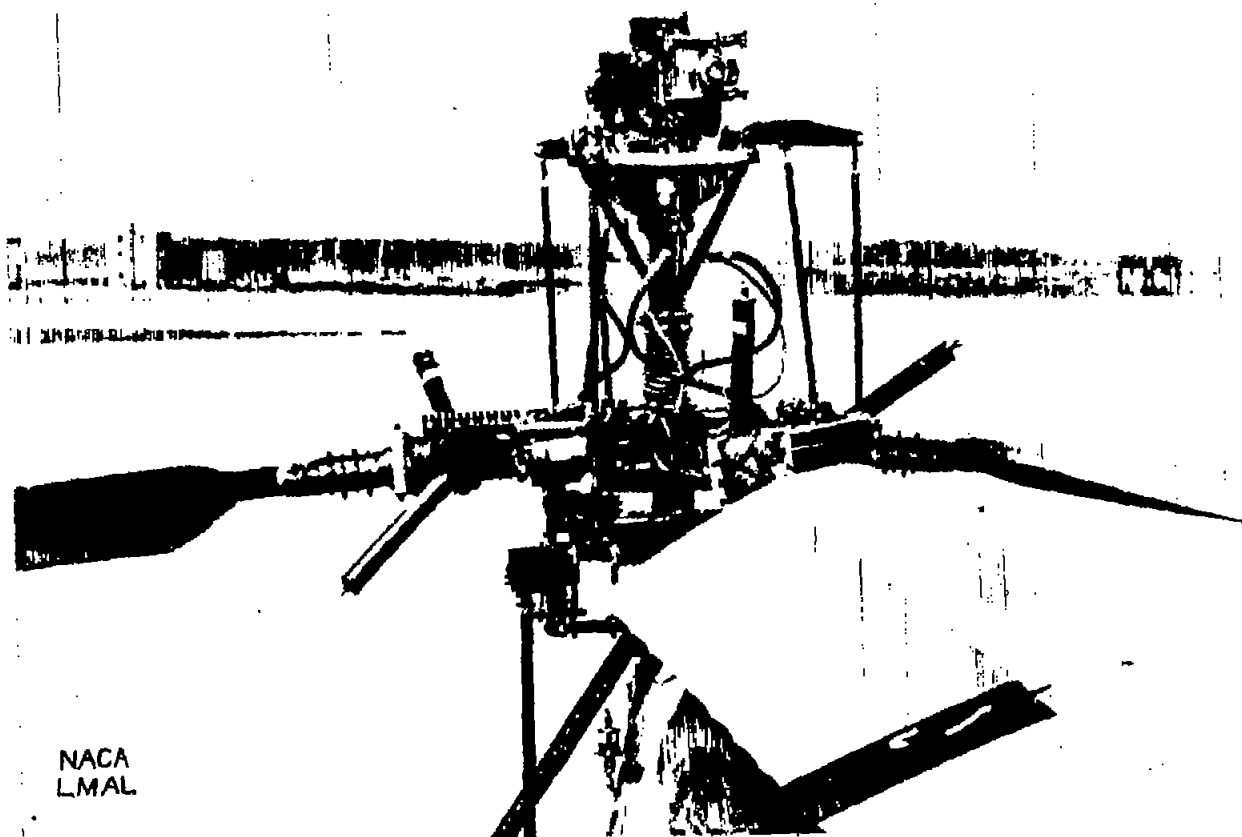




Radius, feet . . . . .	19
Solidity ratio . . . . .	0.06
Airfoil section . . . . .	NACA 0012
Moment of inertia about flapping hinge, slug-feet <sup>2</sup> . . . . .	160.3
Distance of flapping hinge from axis of rotation . . . . .	0
Distance of drag hinge from axis of rotation, feet . . . . .	0.76

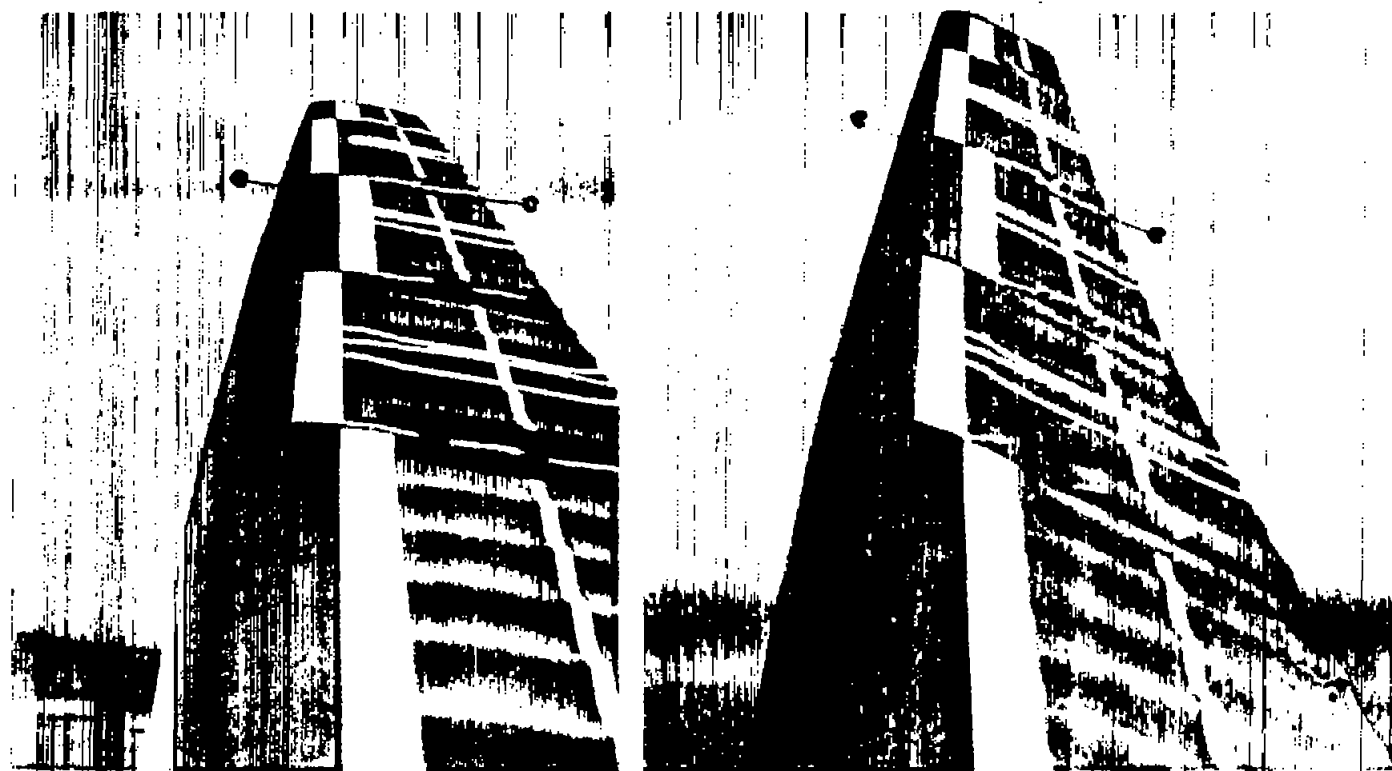
NATIONAL ADVISORY  
COMMITTEE FOR AERONAUTICS

Figure 1.- Physical characteristics of the main-rotor blades. All dimensions are in inches.



NACA  
LMAL

Figure 2.- Camera installation on helicopter rotor hub.



(a)  $\psi = 70^\circ$ .

(b)  $\psi = 310^\circ$ .

Figure 3.- Typical blade photographs taken in flight.

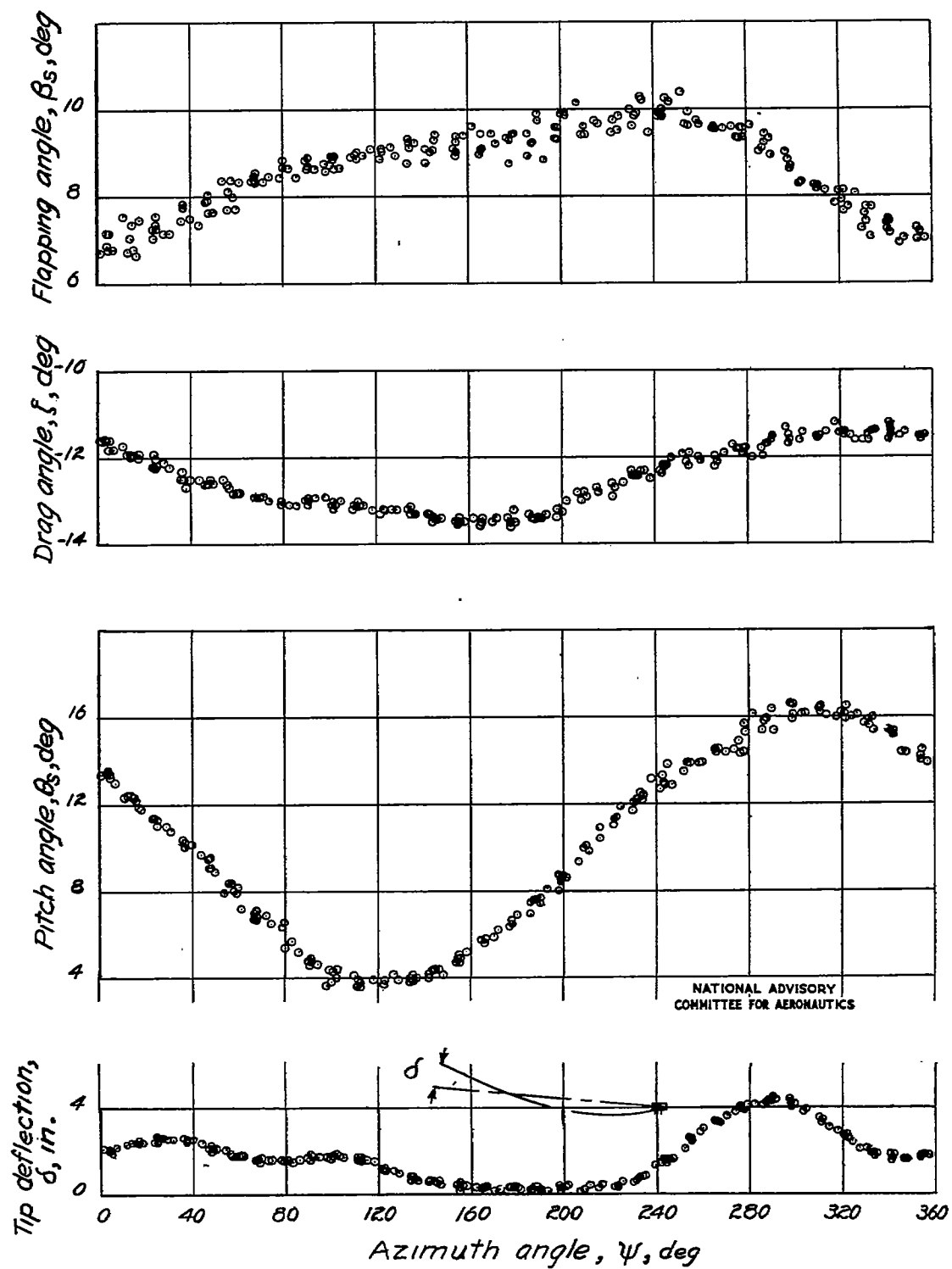


Figure 4.- Sample data obtained from measurements of blade photographs.  $\mu = 0.23$ ;  $C_T = 0.0055$ .

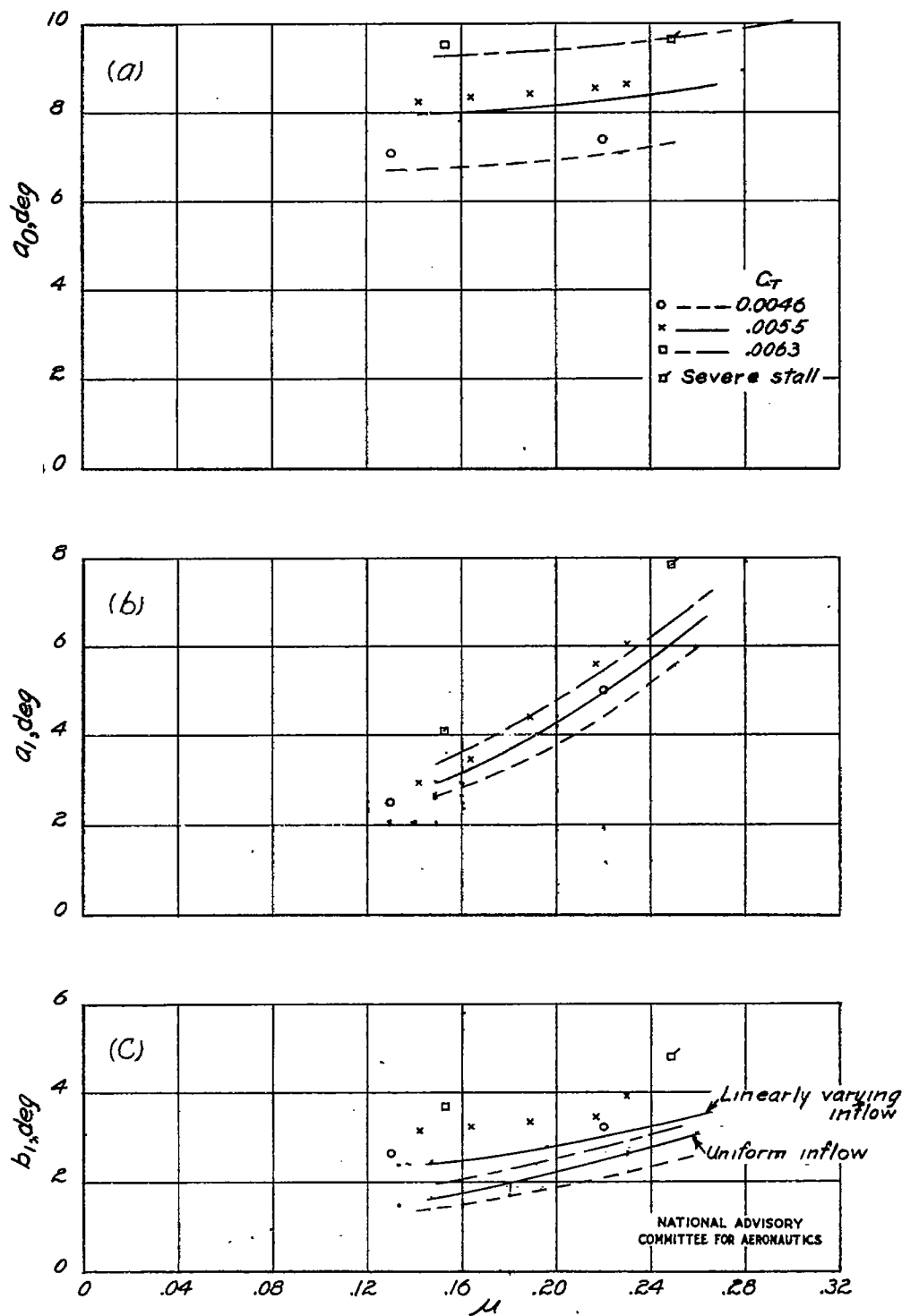


Figure 5.- Comparison of calculated and measured flapping coefficients and pitch angles in level flight.  $\gamma = 12.1$ .

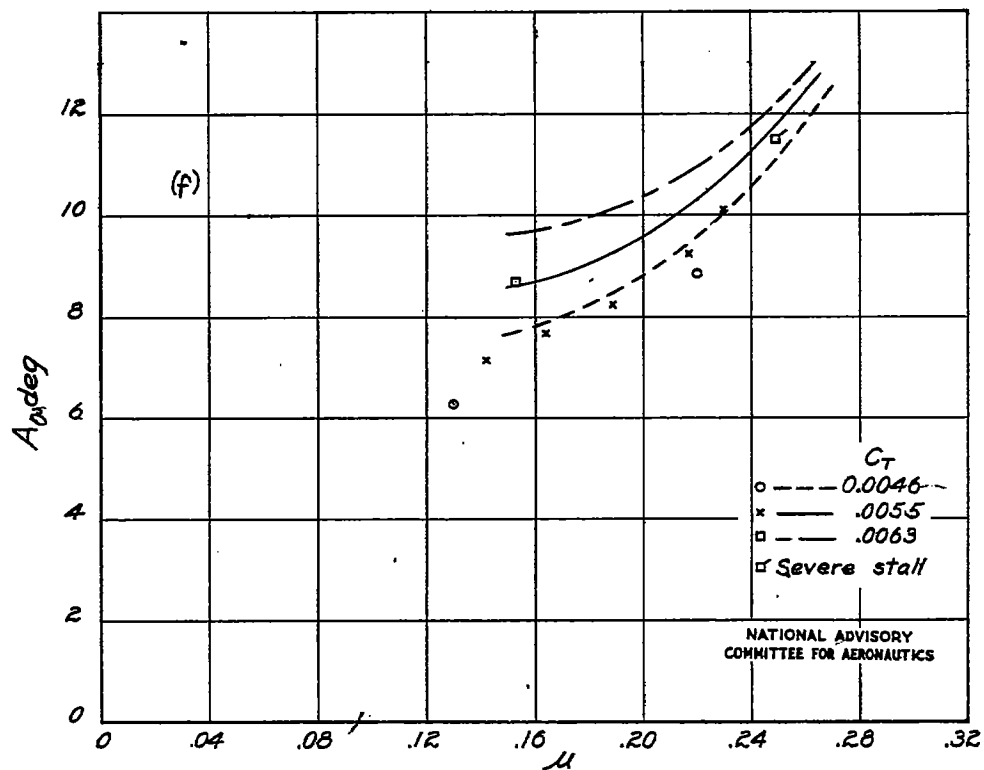
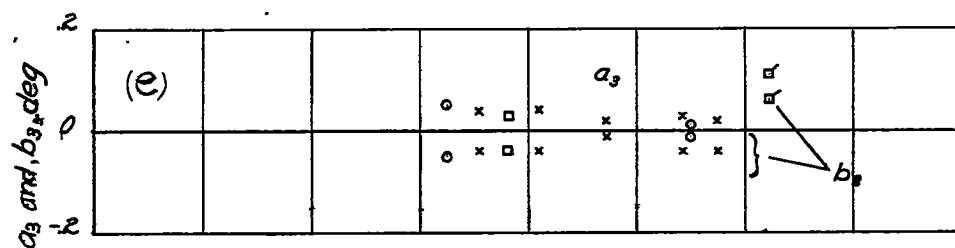
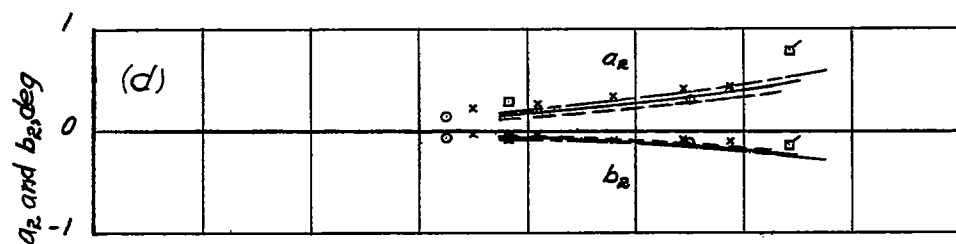


Figure 5.- Concluded.

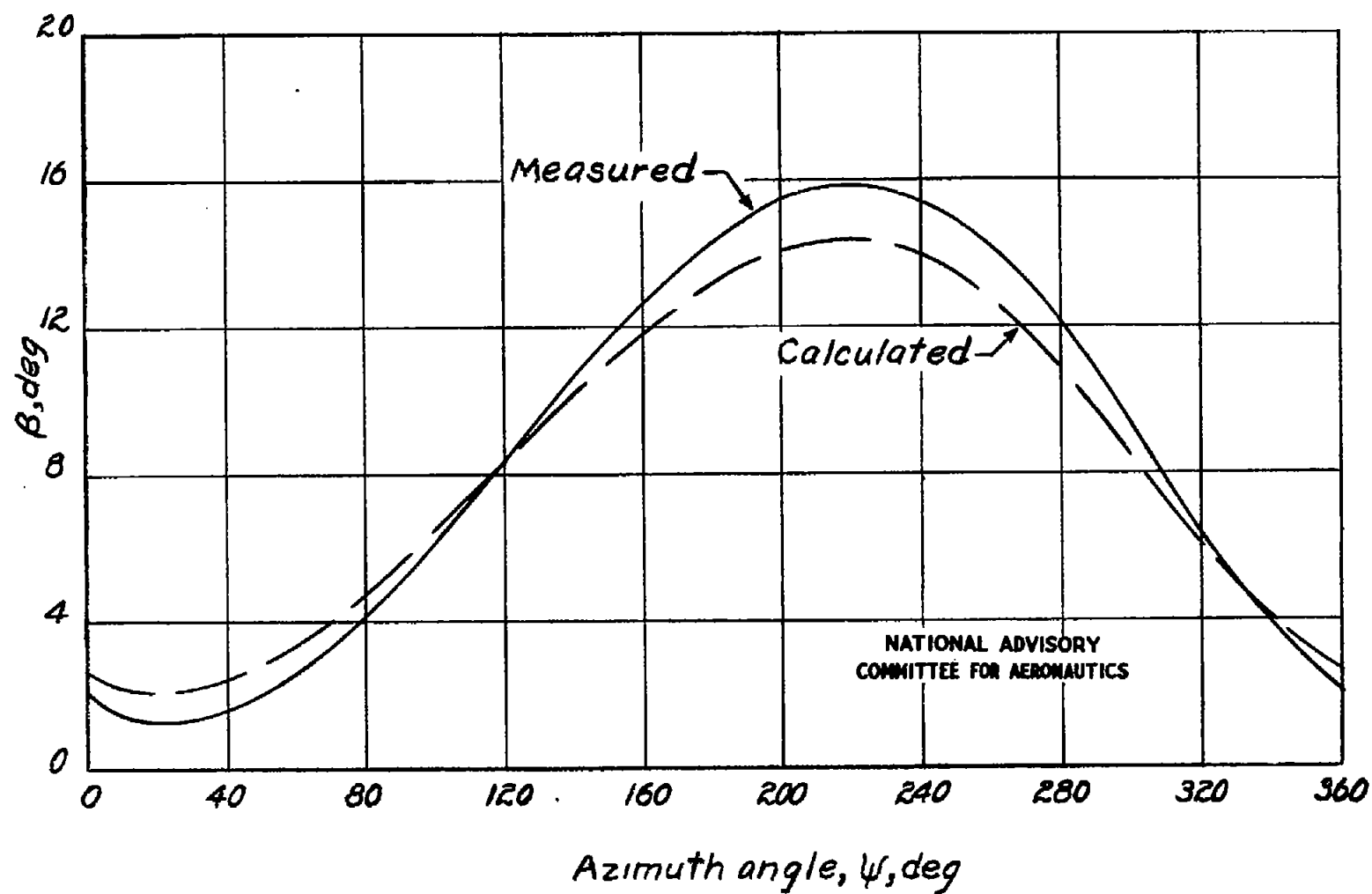


Figure 6.- Experimental and calculated blade-flapping motion  
for  $\mu = 0.23$ .

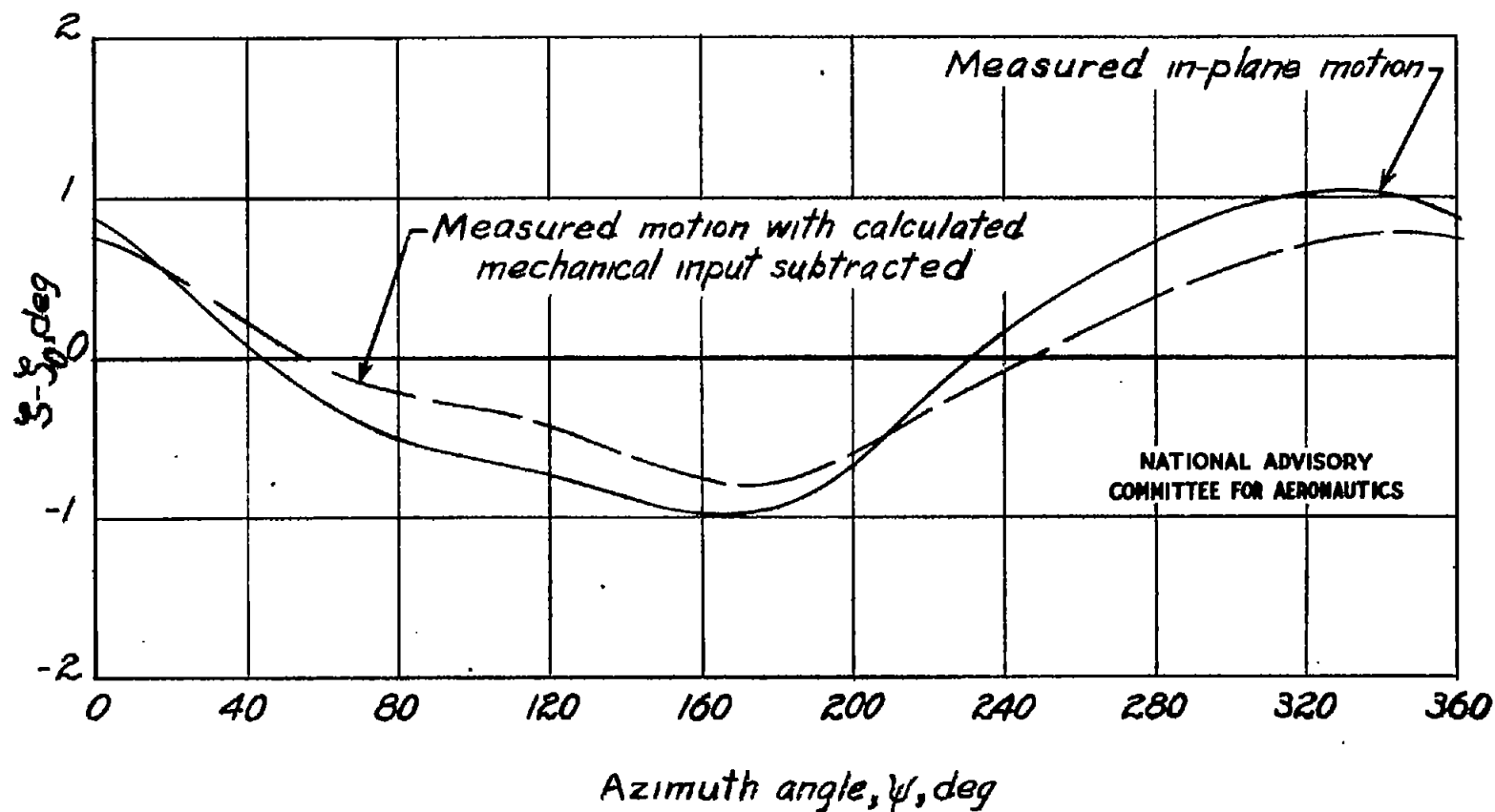


Figure 7.- Periodic portion of in-plane blade motion measured in flight as compared with in-plane motion due to air forces alone.  
 $\mu = 0.23$ ;  $C_T = 0.0055$ .



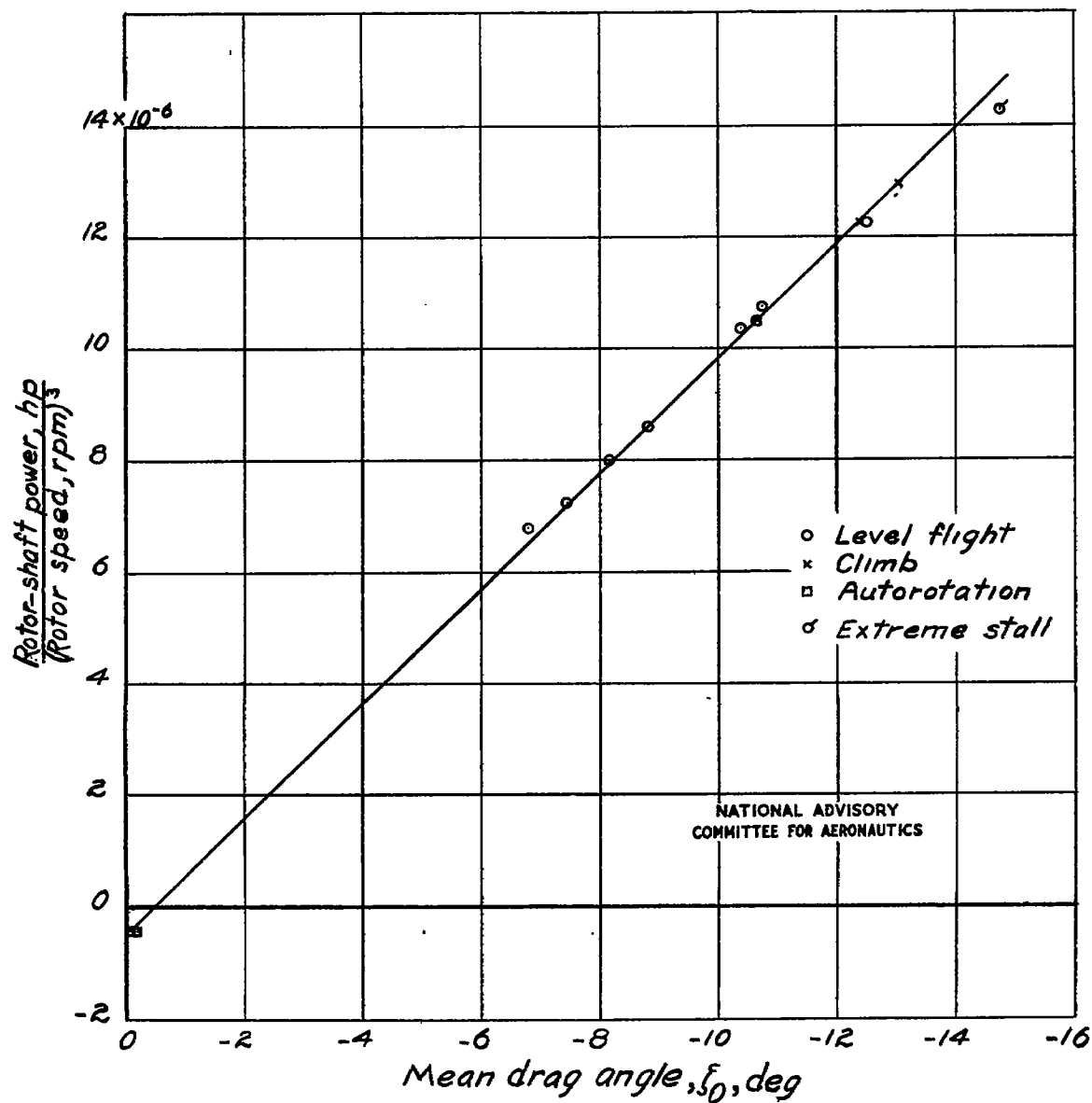


Figure 8.- Measured variation of mean drag angle with ratio of rotor-shaft power to cube of rotor rotational speed for a variety of conditions of flight.

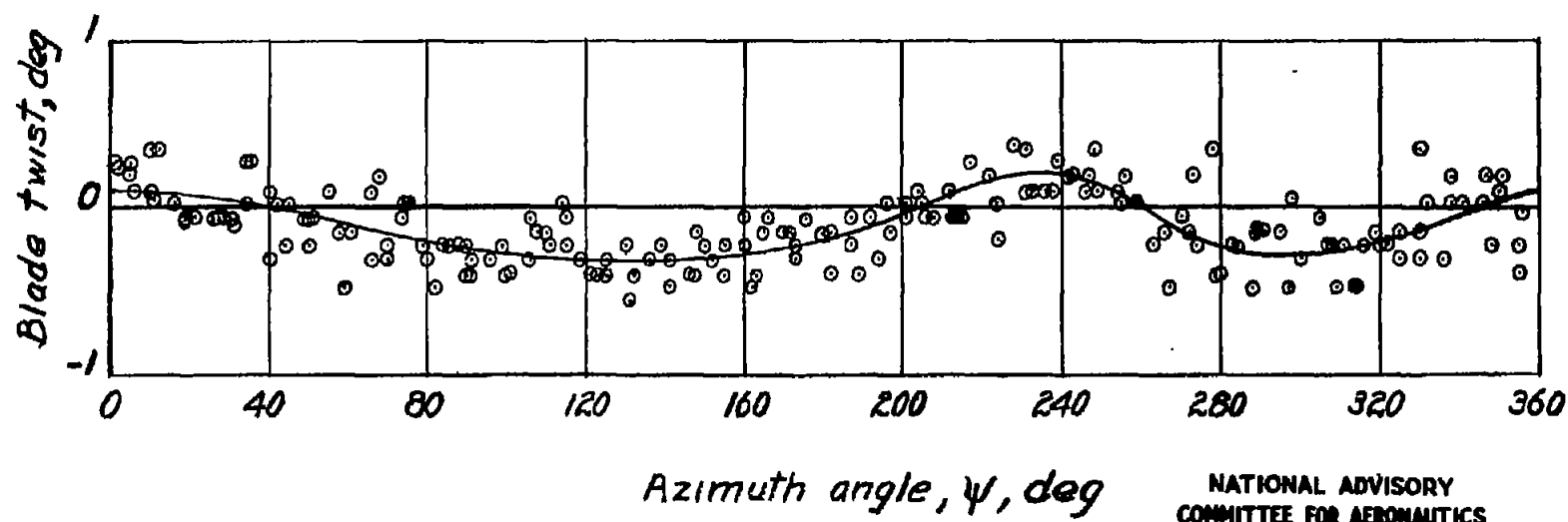


Figure 9.- Blade twist between 0.50 radius and 0.75 radius as measured in flight for a stalled condition.  $\mu = 0.25$ ;  $C_T = 0.0063$ .

Fig. 10

NACA TN No. 1266

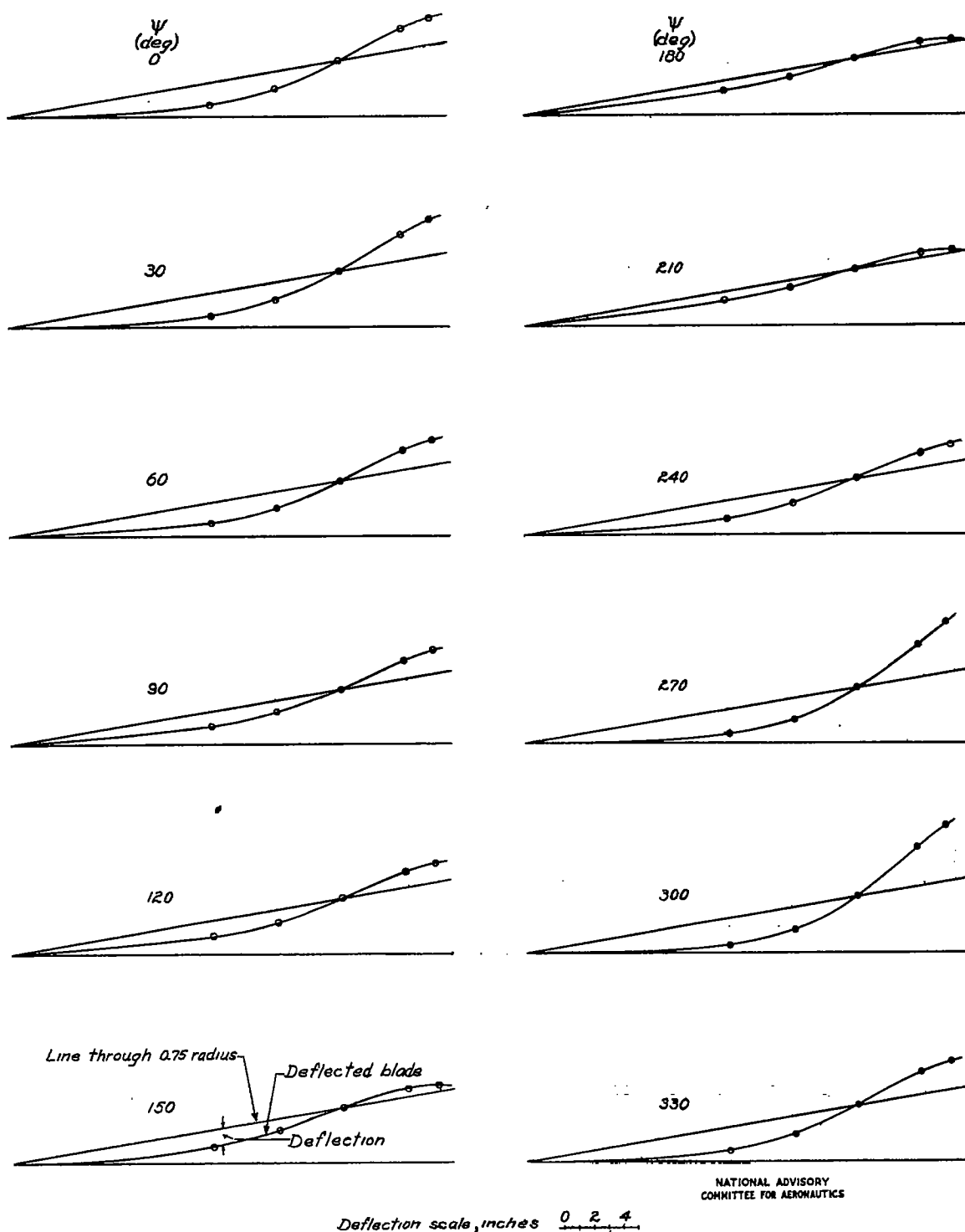
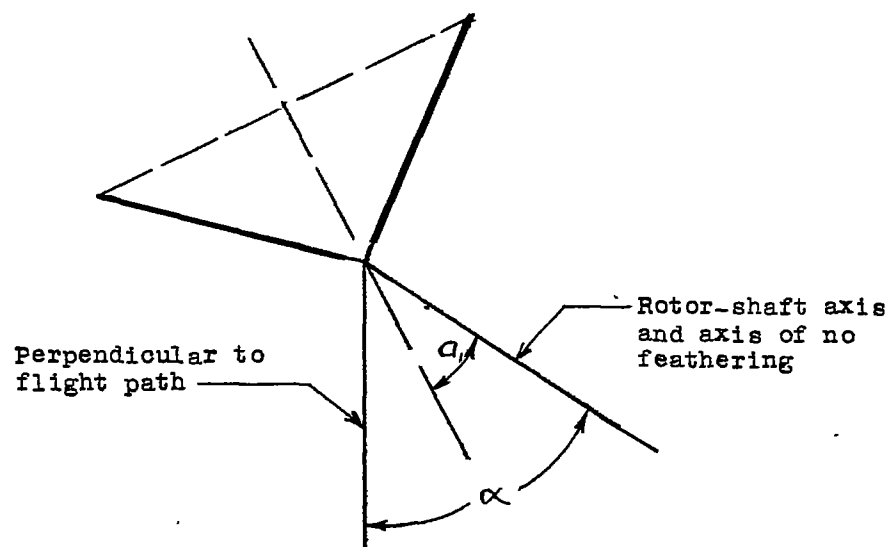


Figure 10.- Blade bending as measured in flight.  $\mu = 0.23$ ;  $C_T = 0.0055$ .



(a) Pure flapping system.

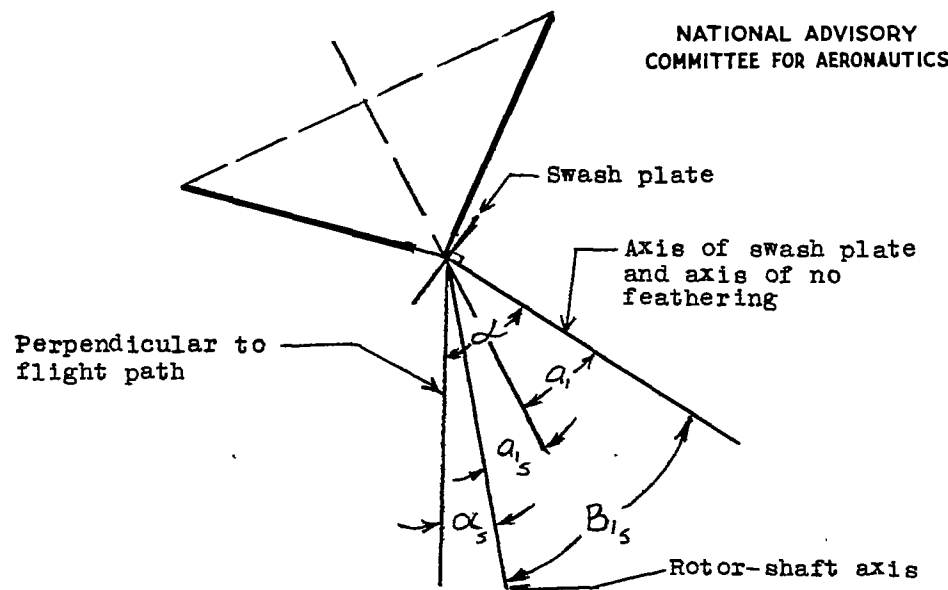


Figure 11.- Longitudinal cross sections of the rotor cone, showing the equivalence of a system involving both flapping and feathering (referred to the shaft axis) to a (pure) flapping system (referred to the axis of no feathering).